Available online at www.sciencedirect.com

SciVerse ScienceDirect

Energy Procedia 24 (2012) 83 – 98

Energy Procedia

Smooth transition between controllers for floating wind turbines

Eivind Lindeberg[a], Harald G Svendsen[b,*], Kjetil Uhlen[c,b]

[a]*Statnett, Oslo, Norway*
[b]*SINTEF Energy Research, Trondheim, Norway*
[c]*Dept. Electric Power Engineering, Norwegian University of Science and Technology, Trondheim, Norway*

Abstract

This paper presents a novel wind turbine control system which gives a smooth power output during transitions between different controllers. The paper presents an implementation of a control system designed for an offshore floating wind turbine using a linear Model Predictive Control approach.

The performance is investigated in computer simulations, with emphasis on stability in the tower fore–aft motion and behaviour during transition between controllers. The results clearly demonstrate that the wind turbine using the proposed algorithm for smooth transition indeed exhibits a smooth system behaviour. In comparison to a case with sudden transition, the behaviour is found to be significantly improved. Moreover, tower oscillations are found to be stable, by virtue of the controller prediction horizon exceeding the natural periodicity of the tower oscillations.

Smooth system behaviour is important to increase the lifetime of critical parts of the turbine. With increasing turbine sizes such considerations are of increasing importance, making the results obtained in this paper of particular relevance for large wind turbines, both onshore and offshore.

Keywords: Offshore wind, wind turbine control, floating wind turbine, model predictive control

1. Introduction

With the development of ever larger wind turbines and the move to offshore installations, an increasing importance is put on the turbine control system. Traditional wind turbine control has primarily been designed to maximise the power output for wind speeds up to the rated speed, and to limit the output for higher speeds in order to avoid damage to the turbine. Simply put, the choice of control system is a balance between simplicity (cost) and the expected increase in lifetime and reduction in maintenance. Small turbines favour a simple and cheap control system, whereas larger turbines may favour more advanced control systems.

Modern, very large turbines are inherently more flexible than traditional ones, and damping of natural oscillations is therefore an important additional objective for the control system. Structural stresses are larger, and the reduction of wear is relatively more important. Moreover, due to the high overall cost of

*Corresponding author
Email address: harald.svendsen@sintef.no (Harald G Svendsen)

 doi:10.1016/j.egypro.2012.06.090

a large turbine, including cost of maintenance and downtime, implementation of a more advanced control system is feasible without affecting the total cost too much. This is even more important for offshore wind farms, where installation and maintenance costs in particular are much higher.

Floating turbines have additional low-frequency oscillatory tower motions, and for these, the turbine control system can be instrumental in ensuring stability.

This paper addresses the issue of control of floating offshore wind turbines, with emphasis on the switching between different controllers. A novel algorithm is presented that ensures a smooth transition (or *bumpless transfer*), which in turn should reduce wear on the turbine and subsequently increase the expected lifetime. The paper presents a simulation model of a floating horizontal axis wind turbine in the 5 MW range, and a control system implementation based on Model Predictive Control (MPC). The smooth transition behaviour is demonstrated through simulations.

1.1. Background

Offshore wind is currently in rapid development, and several large wind farms have already been installed, of which the largest one to date is Thanet (UK) with 300 MW capacity. Present (end of 2010) values for total wind power capacity installed within the EU is 84 GW, of which 2.9 GW is offshore [1]. The wind power industry, and the offshore sector in particular, is set to see a dramatic development in the coming years. The 2020 baseline target by the European Wind Energy Association (EWEA) is 230 GW wind power capacity installed, of which 40 GW offshore wind [1].

So far, all offshore wind farm installations have been in shallow waters (up to approximately 30 m), largely relying on the same technology as for onshore wind farms. In deeper waters new concepts for the foundations have to be developed, and in very deep waters, floating turbines will be the only viable solution. Commercial deployment of floating wind turbines are not expected before 2020.

To date, two floating wind turbines have been installed: *Blue H* is a prototype tension-leg floating platform together with a small 80 kW wind turbine that was installed in 2008 in 113 m water depth off the south-eastern coast of Italy. The turbine was not grid-connected, and was decommissioned in early 2009 after 6 months testing [2]. *Hywind* is a fully operational 2.3 MW spar-buoy floating turbine installed by Statoil off the south-western coast of Norway in 2009. The turbine is currently in operation and is delivering power to the mainland grid [3]. Other concepts for floating wind turbines that are in development include Sway [4], and WindFloat [5].

1.2. Control system objectives

There are several control objectives for a wind turbine. Typically, the overall goal of a wind turbine design is to minimise the lifetime cost of power. In other words, the goal is to simultaneously maximise the power output, maximise the operating lifetime, and minimise the investment cost and need for maintenance. These criteria are to some degree conflicting, so a good balance has to be found.

Details about the control systems in various wind turbines is generally sensitive information that manufacturers tend to keep for themselves. However, most modern variable speed turbines operate according to the same basic principles. See Figure 1. Control regions with different control objectives are defined depending on the wind speed:

I) At low wind speeds below the cut-in speed the turbine is non-rotating.

II) At modest wind speeds the rotational speed of the turbine is controlled so as to give maximum power output based on a power coefficient curve.

III) At high wind speeds when the rotational speed has reached the rated value the turbine is controlled so as to maintain (limit) rated rotational speed. The power is still increasing with wind speed, but at less than optimal efficiency.

IV) At very high wind speeds when the power output has reached rated power the turbine is controlled such as to maintain (limit) the power output. For wind speeds above a certain cut-out limit, the power output is gradually reduced until the turbine is turned off completely to avoid damage.

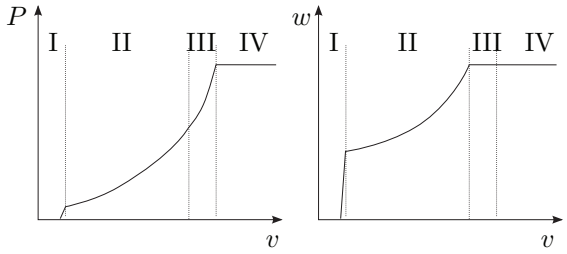

Figure 1: Output power (left) and turbine speed (right) for varying wind speed for a typical variable speed wind turbine. I is the region below the cut-in speed. II is the power maximization region. III is the constant turbine speed region. IV is the power limitation region

In addition to the above primary control objectives, there may be additional concerns for which the control system needs to play an active role, such as active damping of tower fore–aft motion and potential structural eigen-frequencies that cannot be avoided by design choices, reduction of blade flapping of large elastic blades, and active damping of drive-train and generator oscillations. For floating turbines there are low-frequency motion, notably in the fore–aft direction that needs to be limited, that is negatively damped with conventional pitch control. This type of tower motion is discussed in Section 5.1.

At this point it is worth clarifying some matters of language. In this paper, the term *control region* refers to the different operational regions with their different control objectives, as illustrated with an example in Figure 1 and numbered I-IV above. The term *controller* with its associated *controller range* is used to refer to one of several separate controllers designed to be active in a range around a specific operational point (see Figure 3). In the linear MPC approach, multiple controllers are necessary to give an overall good representation of the non-linear dynamics. The controller range should not be larger than the range of validity of the linearisation of the model around the associated operating point. In practice, this means that the control within each control region is typically achieved by one or more controllers.

Smooth transition in this context refers to the smooth transition between different controllers, potentially within the same control region.

1.3. Model predictive control

Model Predictive Control (MPC) is an advanced control method that uses an explicit model of the system to calculate the best control effort. MPC predicts the future behaviour of the system in real-time and chooses the optimal control input from that.

At the core of the MPC controller is an optimisation problem given by an objective function that defines the control objectives together with a set of equations describing the system dynamics and a set of explicit upper and lower bounds on variables. One of the main advantages of MPC is exactly this capability to directly handle system constraints on both input variables and system state variables.

MPC was first developed for use in the chemical industry in the 1980s [6]. It was applied to very slow processes and enabled the controllers to use their detailed plant knowledge to decide the control action. Including knowledge about input constraints and measurement noise made it possible to operate closer to the safety constraints, and this could make the operation more profitable.

Since MPC applies real-time optimisation it requires a lot of computational power. This has previously limited the use of MPC to systems with slow dynamics, but due to the vastly increased speed of computers in recent years, real-time optimisation can today also for fast-changing systems be a viable alternative.

Due to the extra complexity of non-linear MPC, the controller considered in this study is based on a *linear* MPC approach. In this case the controller predicts system behaviour based on a linear control model that usually is a good approximation in a certain range around a chosen operating point. However, since the wind turbine dynamics is highly non-linear, the range of validity for any given linearisation is limited. A drawback with the linear approach is therefore that multiple controllers, each with their different linear control model, must be specified to cover the entire operational range. For the linear MPC approach to be

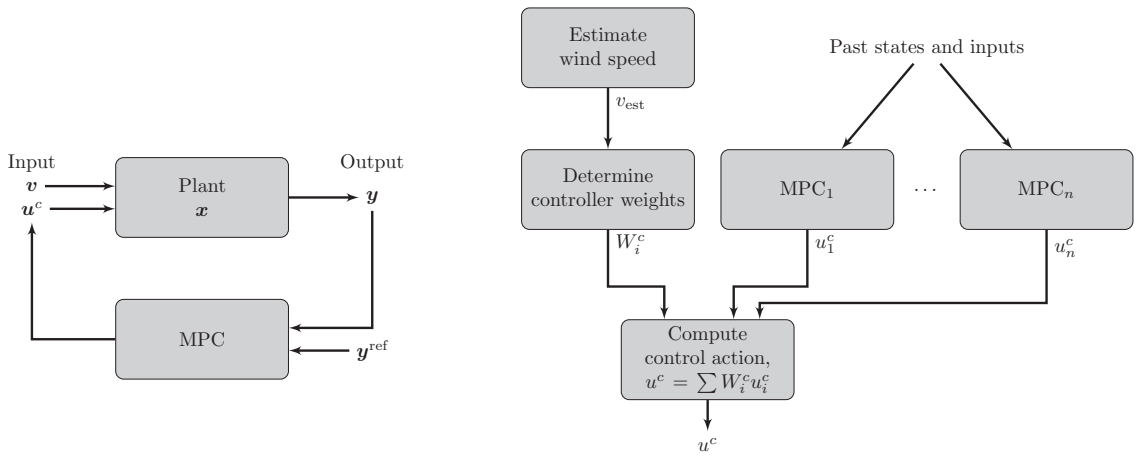

(a) MPC controller

(b) Controller selection algorithm

Figure 2: Schematic representation of the MPC controller (a) and the algorithm that determines the control action (b)

successful, it is a pre-requisite that sufficiently many controllers are defined such that the combination of them together give a good representation of the non-linear dynamics.

A review of MPC is given in ref. [7]. MPC in the context of wind turbine control has been discussed e.g. in refs. [8, 9, 10, 11], and an example of MPC application with wave power is found in ref. [12].

An illustration of the MPC approach is given in Figure 2a. More details about MPC implementation used in this study is given in Section 4.

The remainder of this paper describes an MPC approach to the operational control of a floating wind turbine. Section 2 gives a general discussion of the algorithm that enables bumpless transition between controllers. Then, an overview of the floating wind turbine model is presented in Section 3. Section 4 describes in more detail the implementation of the MPC based controller. Section 5 presents simulation results where the developed controller is tested under different circumstances. Finally, Section 6 offers some concluding remarks.

2. Bumpless transfer

A floating wind turbine is a very non-linear system and this impedes the use of *one* linear control model for the entire operational range. Also, different operating points may have different control objectives and require different control strategies. To overcome these problems, different controllers can be designed around different operating points, together with an algorithm that determines how the control action is deduced from the output of the various controllers.

Because the MPC approach uses past states and control inputs to estimate the system state and to calculate the optimal future input sequence, the controller can not be "cold started", i.e. it has to run and be aware of both the actual input and the measurements before it is made active. This achieved by letting each controller be running sufficiently far outside its controller range, accounting for potential rapid changes in wind speed. If computational power is not a limitation, all controllers can be running in parallel all the time, avoiding this issue altogether. Even when the controller is running, a sudden transfer from one controller to the other is likely to cause sudden changes in control actions that may result in rapid changes or spikes in the power output. This in turn has a negative effect both on the turbine lifetime, and on the power quality. In

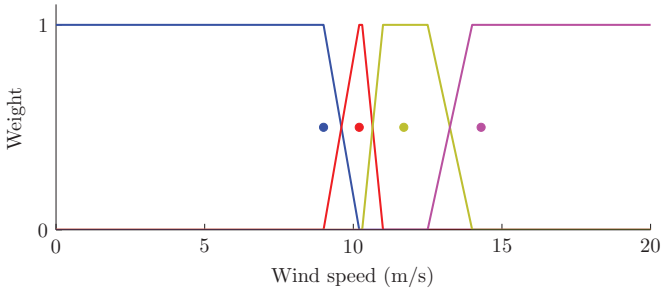

Figure 3: Illustration of controller weights (lines) and wind speeds used for linearisation (dots).

order to reduce such effects, this paper proposes a gradual switching between controllers based on estimated wind speeds.

The gradual switching is obtained by assigning *weights* W_i^c to the different controllers and defining the overall control input u^c as the weighted sum of control inputs u_i^c determined by the separate controllers:

$$u^c = \sum_{i=1}^{n_c} W_i^c u_i^c, \tag{1}$$

where n_c denotes the number of controllers. This approach is illustrated in Figure 2b. The weights always add up to one, and depend on the estimated wind speed, as illustrated in Figure 3.

The wind speed estimate is derived from measured values of power P, blade pitch angle β and rotational speed ω_t, and acceleration $\dot{\omega}_t$: Considering the entire drive-train including rotor as a single mass with rotational inertia J, by conservation of energy, the difference in aerodynamic power and electric power equals the change in rotational kinetic energy.

$$P_w - P_e = \frac{d}{dt}(\frac{1}{2}J\omega^2) = J\omega\dot{\omega}. \tag{2}$$

Using the relationship between wind power and speed given in equation (4), we get the following expression for the wind speed which can be used to estimate instantaneous wind speed from measured values of more easily accessible variables:

$$v_{\text{est}} = \left(\frac{P_e - J\omega\dot{\omega}}{\frac{1}{2}A\rho C_p(\lambda,\beta)}\right)^{\frac{1}{3}}. \tag{3}$$

This is a simple approach to estimating the wind speed, but since the objective of the present study is not to optimise the controller, but rather to demonstrate the control philosophy, the errors induced by the wind estimate are not considered crucial. However, it should be acknowledged that, since the controller depends on the wind estimate, it is sensitive to such errors, and having a poor wind estimator inevitably gives non-optimal control system behaviour, especially if the controllers in neighbouring controller ranges are very different. Due to this sensitivity, it is advisable to have robust controllers especially around rated wind speed where the control objectives can change considerably even for a small shift in the operating point. The implementation of more advanced and reliable wind estimation could remedy this weakness, but is considered outside the scope of the present study.

To summarise, the novelty of the controller outlined above is that the transition between controllers is not simply on-off, but gradual and specified by weight as illustrated in Figure 3.

3. Floating wind turbine model

This section gives a brief description of the simulation model used for testing the control system outlined above. The model is formulated as a modestly detailed non-linear physical model. A more detailed description of the model is found in ref. [13].

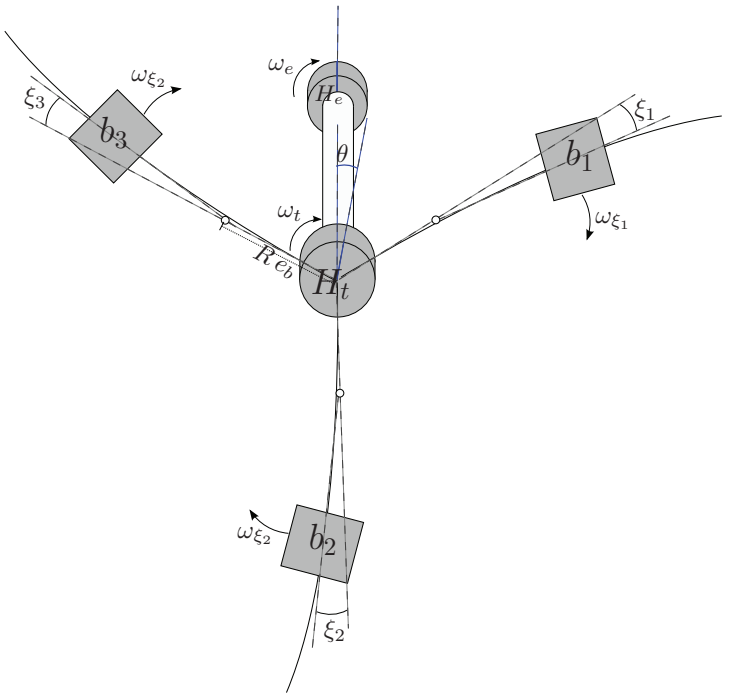

Figure 4: Schematic drawing of the five mass model of the wind turbine, showing a lump mass for each blade, and the 2-mass drive-train.

The floating wind turbine that is modelled is a standard 3-bladed horizontal axis wind turbine mounted on a floater, resembling the Hywind concept [3]. The wind turbine is described as a 5-mass model, as illustrated in Figure 4. The floater, including the tower, is modelled as a stiff body with six degrees of freedom (6 DOF): The linear position in three dimensions (x, y, z) and rotational angle around the three axes.

3.1. 5-mass wind turbine model

Wind power P_w extracted by a wind turbine, and the wind thrust force F_T on the tower are commonly expressed by the equations

$$P_w = \frac{1}{2} A \rho C_p(\lambda, \beta) v_r^3, \tag{4}$$

$$F_T = \frac{1}{2} A \rho C_t(\lambda, \beta) v_r^2. \tag{5}$$

where A is the area swept by the wind turbine blades, v_r is the effective wind speed, ρ is the air density, and the power efficiency coefficient $C_p(\lambda, \beta)$ and thrust coefficient $C_t(\lambda, \beta)$ are non-linear maps from the tip speed ratio λ and blade pitch angle β. These coefficients depend on the design of the turbine, and for the purpose of control design these are often specified in terms of look-up tables.

The 5-mass model of the turbine includes a lump mass for each of the three blades together with a standard 2-mass representation of the drive-train, see Figure 4.

The individual blade motion is modelled as a stiff hinge, and is described by 2 degrees of freedom as in-plane and out-of-plane bending. For the purposes of investigating the transition between controllers, however, the detailed blade modelling is not important and is therefore not elaborated on any further in this paper. Likewise, independent blade pitching was originally assumed in the simulation model in order to address blade vibrations, although this is not in focus of the present paper. It is assumed that a control system with collective pitch would not alter any of the findings presented here.

Table 1: Basic floater data

Radius	5 m
Height	100 m
Weight	7200 t
Centre of gravity (including turbine)	−80 m
Eigenfrequency in pitch	41.3 s

The blade dynamics is coupled with the dynamics of the drive-train. As stated above, the drive-train is modelled as a 2-mass model with the hub mass (including blades) at one end, the generator mass at the other, and a spring and damper connecting them.

The generator in the offshore wind turbine discussed here is assumed to be a permanent magnet synchronous generator. The dynamics of the generator is much faster than the drive train dynamics. Ref. [14] indicates that the power control system gives settling times of around 0.01 s, i.e. $f \approx 100$ Hz. For the slower dynamics of the wind turbine we can therefore assume that the electric power output equals the setpoint power, $P_e = P_{\text{set}}$.

Wind time series used in the simulations are generated using a turbulence model based on the von Kármán spectrum, using the rational transfer function approximation suggested in ref [15] (equation 25). In addition to turbulence, the wind time series also account for wind shear and tower shadow, by interpolating between four different time series representative of four different blade positions (up, left, down, right).

3.2. Floating platform model

The wind turbine is assumed to be mounted on a long and slender, cylindrical floater. It is furthermore assumed to be very massive and have a low centre of gravity in order to make the entire structure, including the turbine, stable. The floater design has been chosen to resemble the Hywind concept [3]. The basic data for the floater is given in Table 1.

The 6 DOF model of the floater is obtained from WAMIT [16], a high-end numerical potential theory program that can produce the vessels dynamic equations and wave response. The input to WAMIT is the size, shape and weight of the structure. The output can be used to formulate a first order dynamical model of the floater. The external forces in this model are the wind thrust and the wave forces.

The tower motion and the blade motion induces movement at the blades that leads to a change in the experienced wind speed. The effective wind speed v_r can be expressed as

$$v_r = v + v_m, \tag{6}$$

where v is the actual wind speed, and v_m is speed due to structural motion.

The wave model that is used in the simulations is based on *Wave Force Response Amplitude Operators* as described in ref. [17]. They are computed with WAMIT together with the floaters dynamical equations.

In the simulations the wave height is derived from the mean wind speed and the Beaufort scale. The peak frequency is chosen to be 0.8 rad/s, which is indicated as a typical value in ref. [17].

It is important to note that the common wave frequencies are higher than the eigenfrequencies of the floating platform. This is achieved by design choices for the floating wind turbine.

3.3. Linear control model

The implementation of an MPC controller requires a linear control model, which is obtained from the model outlined above through a reduction and standard linearisation procedure. A good (piecewise) linear representation of the entire operational range can only be achieved by multiple linear models based on linearisation around different operating points. Hence multiple MPC controllers must be defined.

The gravitational forces on the blades are large and lead to a dominant movement of the blades with frequency equal to the rotational frequency. It is clearly not desirable (nor possible) to damp out these fluctuations. This frequency therefore needs to be filtered out from the measurements when designing the

controller. This can be done with a band-stop filter filtering out the rotational frequency, or with a feed forward connection from the rotor azimuth position.

The reduced turbine model has four control inputs: one for each blade pitch set-point and one for the generator set-point. The 6 DOF model of the floater is reduced to 3 DOF by assuming no sway (sideways motion), no roll (sideways rotation), and no yaw (rotation around vertical axis). The main justification for this reduction is that the dominant tower motion is the fore-aft (pitch) motion, which is negatively damped with conventional blade pitch control.

The wind speed at each blade is considered a disturbance and so is the wave influence on the floater.

The full dynamical system can be expressed in the standard first order form

$$\dot{\boldsymbol{x}} = f(\boldsymbol{x}, \boldsymbol{u}), \tag{7}$$

where $\boldsymbol{x}$ is the *state vector* and $\boldsymbol{u} = \{\boldsymbol{u}^c, \boldsymbol{v}\}$ is the *input vector*. The state vector contains variables that fully determine the state of the system. The input vector consists of two parts, the *control vector* $\boldsymbol{u}^c$ which contains controllable variables, and the *disturbance vector* $\boldsymbol{v}$ which contains other input variables over which the control system has no influence.

With this starting point, the system of equations is linearised in standard fashion around an operating point $(\boldsymbol{x_0}, \boldsymbol{u_0})$, and then discretised to give an equation on the form

$$\boldsymbol{x}(k+1) = A\boldsymbol{x}(k) + B\boldsymbol{u}(k), \tag{8}$$

where k denotes a discrete time, and A and B are matrices determined by system properties.

The control action depends on the value of certain output variables $\boldsymbol{y}$ and their associated reference values $\boldsymbol{y}^{\text{ref}}$. With an appropriate choice of coefficient matrices C and D these output variables can be written as

$$\boldsymbol{y}(k) = C\boldsymbol{x}(k) + D\boldsymbol{u}(k), \tag{9}$$

4. Turbine control

4.1. MPC approach

The basic idea of MPC is at every time step to predict the future system behaviour given the current system state for some future sequence of control inputs. Control actions are found through an optimisation procedure formulated in terms of an objective function and a set of constraints. This objective function typically includes state errors and control effort. The control input for the first time step is applied to the function, and the procedure is repeated before the next time step.

Figure 5 illustrates the operation of the MPC controller at a discrete time k. The top plot shows the state $\boldsymbol{x}$. The blue line on the left of time k represents the measurements, and the predicted optimal output sequence on the right of time k. The black line represents the resulting actual system state. The reference trajectory is shown in the lower plot. Note that only the first control action, marked with a heavy black line, is actually applied to the system, because the complete procedure is performed again at time $k+1$. H_c and H_p denote the control and prediction horizon respectively. The control horizon is how many time steps the control action is allowed to vary in the prediction, and the prediction horizon is the number of time steps included in the optimisation.Typically $H_p \gg H_c$.

Some basic simulation parameters are shown in Table 2.

As noted previously, the model is linearised around multiple points to properly represent the overall non-linear behaviour of the full system. This gives rise to multiple controllers that have different parameters, including different weights in the objective function and different constraints.

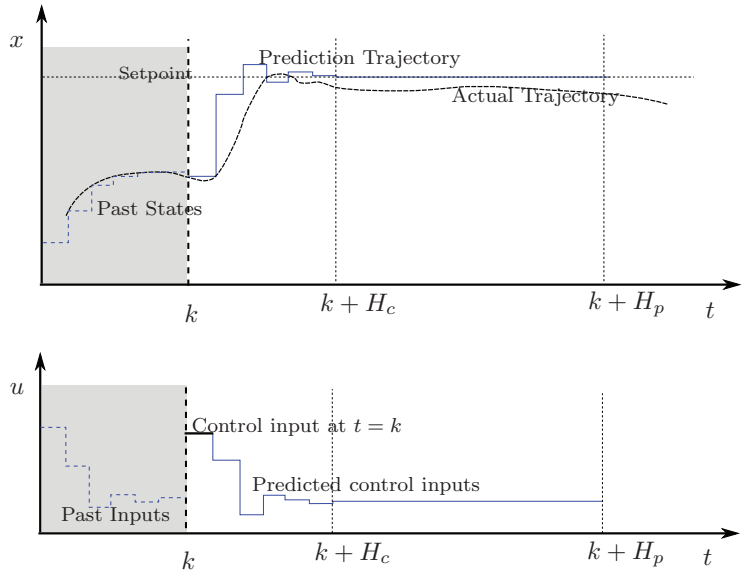

Figure 5: Illustration of the basic concept of predictive control. The top plot shows the development of the system states, while the lower plot shows the control inputs.

Table 2: MPC parameters

Time step (s)	$T_s = 0.25$
Control horizon	$H_c = 15$
Prediction horizon	$H_p = 200$

4.2. Control system implementation

The system is modelled in Matlab/Simulink, using the Model Predictive Control Toolbox. Hydrodynamics is implemented using the MSS toolbox [18]. Four different operating points (9, 10.2, 11.7, 14.3 m/s) have been chosen to derive four control models for four distinct MPC controllers, as explained above.

The wind turbine system has a large dynamic range. There are fast, and even unstable, dynamics in the drive-train, while the tilt frequency of the tower has very slow dynamics. These characteristics are important for the controller implementation: The controller time step size must be smaller than the dynamics of the unstable dynamics of the drive train, and the prediction horizon must be large enough to capture the dynamics of the tower.

The MPC controllers are tuned by adjusting objective function weights W in equation (10) and by specifying constraints.

The objective function J associated with an MPC controller specifies the control objectives. In general, this function is a sum of multiple objectives with different weights. It can be written as

$$\begin{aligned} J = \sum_{i=0}^{H_p-1} \Big(\sum_{j=1}^{n_y} |W_j^y (y_j(k+i+1) - y_j^{\mathrm{ref}}(k+i+1))|^2 \\ + \sum_{j=1}^{n_u} |W_j^{\Delta u} \Delta u_j^c(k+i)|^2 + \sum_{j=1}^{n_u} |W_j^u (u_j^c(k+i) - u_j^{\mathrm{ref}}(k+i))|^2 \Big), \end{aligned} \tag{10}$$

where n_u is the number of control variables, and n_y is the number of output variables, $\Delta u_j^c(k) = u_j^c(k) - u_j^c(k-1)$, and W_j are weights which determine the relative importance of different control objectives.

Three classes of control objectives are included in the expression above: 1) output variable reference tracking, 2) control effort (change in control input value), and 3) control variable reference tracking.

The output from the optimisation is the set of control variables $\{u_j^c(k_i)\}$ for $j = 1, \ldots, n_u$ and $k_i = k, k+1, \ldots, k+H_c$.

In our example, the control vector $\boldsymbol{u}^c$ and output vector $\boldsymbol{y}$ are given as

$$\boldsymbol{u}^c = [\beta_1^{\mathrm{set}}, \beta_2^{\mathrm{set}}, \beta_3^{\mathrm{set}}, P^{\mathrm{set}}], \tag{11}$$

$$\boldsymbol{y} = [\theta, \omega_{\xi_1}, \omega_{\xi_2}, \omega_{\xi_3}, \nu_\Theta], \tag{12}$$

where β_i^{set} are the pitch angle set points (for each blade), P^{set} is the power set-point, θ is the drive-train lag angle (twisting of the drive-train), ω_{ξ_i} is the rotational speed of each blade, and ν_Θ is the tower angular fore–aft tilting speed (pitch motion speed). The drive-train lag angle, θ, may not be easily measure directly, but it is assumed here that its value can otherwise be derived indirectly from other measurements.

The reference values $\boldsymbol{y}^{\mathrm{ref}}$ associated with the output variables are

$$\boldsymbol{y}^{\mathrm{ref}} = [\theta^{\mathrm{ref}}, \omega^{\mathrm{opt}}, \omega^{\mathrm{opt}}, \omega^{\mathrm{opt}}, 0], \tag{13}$$

where ω^{opt} is the optimal rotational speed and θ^{ref} is the equilibrium shaft/generator lag angle.

The objective function weights for the different controllers are shown in Table 3. Which are the best choices for the weights depends on the importance of the different objectives, i.e. how much a deviation from the reference value should be penalised. This again depends on the operational region where the given controller belongs, and also on overarching priorities set by the wind turbine operator. The values presented in the table and used in this paper are largely based on tuning through a "trial and error" approach, with no claim that these represent a best choice in any way. Some comments, however, may illustrate the thinking behind the choices: Stabilising the tower fore–aft motion is important in high winds when the pitch regulator is active (see Section 5.1). This is reflected in the value of W_{ν_Θ}. Also, high winds correspond to the constant power output region, so $W_{P^{\mathrm{set}}}$ has a high weight for controller 4.

As mentioned previously, one of the advantages of the MPC approach is that variable constraints are directly taken into account in the optimisation.

Table 3: Objective function weights for the different controllers

Variable	MPC 1	MPC 2	MPC 3	MPC 4
$W_{\beta^{\text{set}}}$	3	1	0.5	0.1
$W_{P^{\text{set}}}$	1	40	100	200
$W_{\Delta\beta^{\text{set}}}$	0.5	0.5	0.5	0.2
$W_{\Delta P^{\text{set}}}$	20	40	2	0.2
W_{θ}	2	2	2	2
$W_{\omega_{\xi}}$	100	100	100	100
$W_{\nu_{\Theta}}$	0	20	50	50

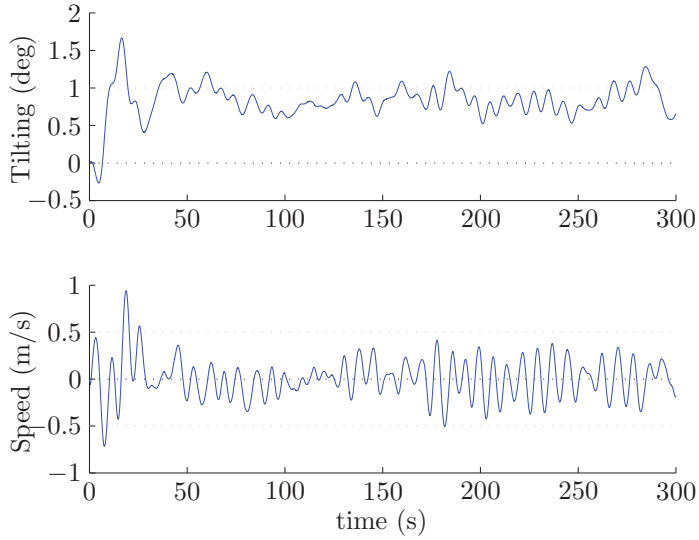

Figure 6: Tower tilt angle and nacelle speed in an average wind speed of 16 m/s.

The constraints used in our model are shown in equation (14).

$$\begin{aligned} 0 \leq\ & P^{\text{set}} \leq 1.0 \text{ pu}, \\ -0.5 \text{ pu/s} \leq & \Delta P^{\text{set}} \leq 0.5 \text{ pu/s}, \\ 0 \leq\ & \beta_i^{\text{set}} \leq 25^{\circ}, \\ -3 \text{ }^{\circ}\text{/s} \leq & \Delta\beta_i^{\text{set}} \leq 3 \text{ }^{\circ}\text{/s}, \\ \omega_s^{\text{min}} \leq\ & \omega_s \leq 1.1 \text{ pu}, \end{aligned} \tag{14}$$

where ω_s is the generator rotational speed, and $\omega_s^{\text{min}} = 0.3$ pu for controllers 1–3, and 0.9 pu for controller 4 (constant speed region).

5. Simulation results

This section presents simulation results addressing the issue of tower stability, which is a basic challenge with floating wind turbines, and the issue of smooth transition between controllers using the approach described in earlier sections.

5.1. Tower motion

With classic wind turbine control, the floating tower motion in the fore–aft wind speed direction (pitching) becomes unstable due to positive feedback: At high wind speeds the wind turbine is in the power limitation region, regulated via pitching of the blades. But blade pitching also affects the thrust force on the tower. When the tower oscillates away from the wind, effective wind speed decreases, and the blade pitching is adjusted to keep the power at the maximum value. This in turn increases the wind thrust force, making the tower move even faster away from the wind. In other words, traditional wind turbine control gives negative damping of tower oscillations.

Different solutions to this issue have been proposed in the literature [19, 20, 21, 22, 23, 24, 25, 26, 27], and operational experience from the Hywind demo have lead the operations and maintenance team to conclude that, with its stabilising control solution, the resulting floater motions have no negative impact on turbine performance [28].

The present MPC-based solution achieves fore–aft tower stability by ensuring that the prediction horizon in the MPC controller is long enough to capture tower oscillations.

Figure 6 shows tower tilt and nacelle speed in a situation with a high average wind speed. The figure shows that the tower is tilted away from the wind with an average value of just under 1 degree. There are small fluctuations in the tilt angle, but there is no sign of the positive feedback instability described above. That is, the control system does indeed stabilise tower motions.

5.2. Bumpless transfer

The control system is designed to work for all wind speeds, and this is achieved by switching between controllers tuned for different operating ranges. As explained in Section 2 a gradual shift from one controller to another ensures smooth system behaviour during these transitions.

In order to test this bumpless transfer algorithm, simulations have been run with different wind speed time series. Figure 7 shows an example using an average wind speed of 10.2 m/s. The top plot shows output power. For the highest wind speeds the power output reaches the maximum (rated) value. As desired, the power output is relatively smooth.

The second plot shows turbine rotational speed (in blue) plotted against the set-point speed (black). Except for some deviations when the set-point is at the maximum speed value, the set-point tracking is good. Small speed deviations as seen in this simulation indicates that the turbine is allowed to speed up or down to absorb rapid wind speed fluctuations. This in turn helps in keeping a smooth power output and reduces structural stresses.

The third plot shows the controller weights. The weights are specified as functions of (estimated) wind speed as shown in Figure 3. The figure shows that for most of the time in this example, the turbine is in a transition region where more than one controller is active.

The bottom plot shows the wind speed (in blue) and the estimate made by the controller (in black). Stochastic fluctuations have been added to give a realistic wind speed time series. As the figure shows, the estimated wind speed is a smoothed curve that follows the actual wind speed well. As noted previously, this is important because the bumpless transfer algorithm uses the estimated wind speed as input.

All in all, these plots demonstrate that the performance of the turbine is not compromised when changing from one controller to another. The turbine speed tracking is acceptable and power output is relatively smooth. The most dramatic behaviour is seen at around 210 seconds, when there is a drop in wind speed corresponding to a relatively rapid change from controller 3 to controller 2 and 1, as is clear from the controller weight plot. It is likely that the behaviour in this case could have been improved by a better tuning of the control system.

To get an indication of the effect of the bumpless transfer algorithm, an identical simulation without this feature has been run. In this case, the weights are either 0 or 1, with a sudden change from one controller to another. The resulting turbine speed and power output is shown in Figure 8. The result in this case is clearly a much less smooth behaviour. The power dip at about 210 seconds mentioned above is now much more pronounced. Additionally, there are are several upwards and downward power spikes where the first simulation gave smooth behaviour. These spikes correspond directly to sudden changes of controllers.

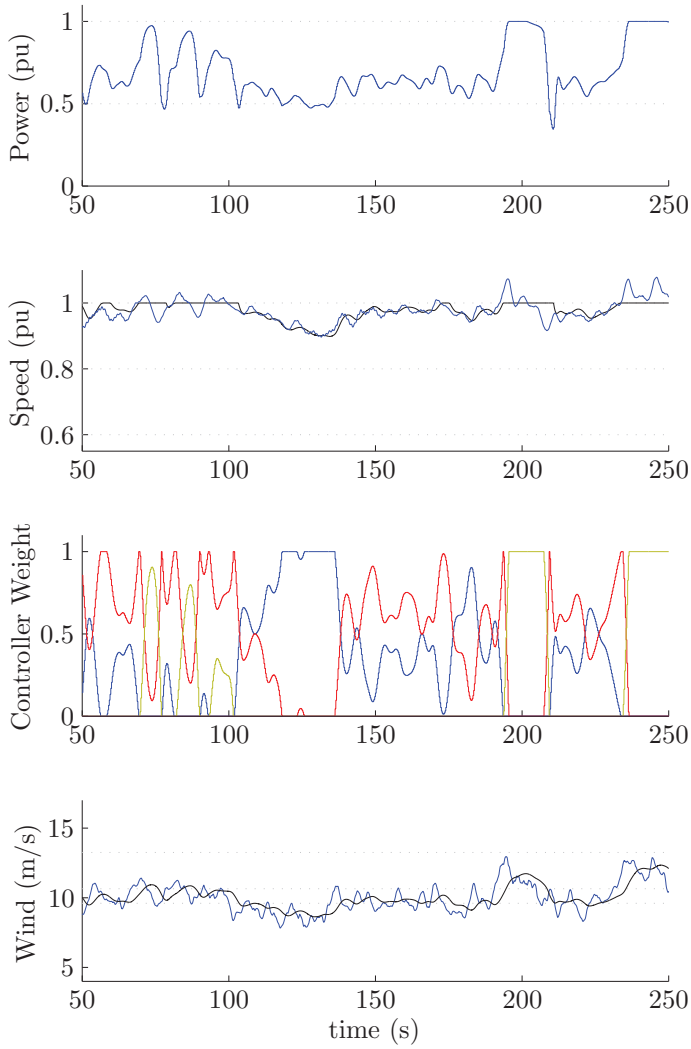

Figure 7: Simulation of wind turbine with smooth transfer between controllers. From the top: 1: Output power; 2: Turbine rotational speed (blue) and speed set-point (black); 3: Controller weight (different controllers are shown with different colours); 4: Average wind speed (blue) and estimated wind speed (black)

.

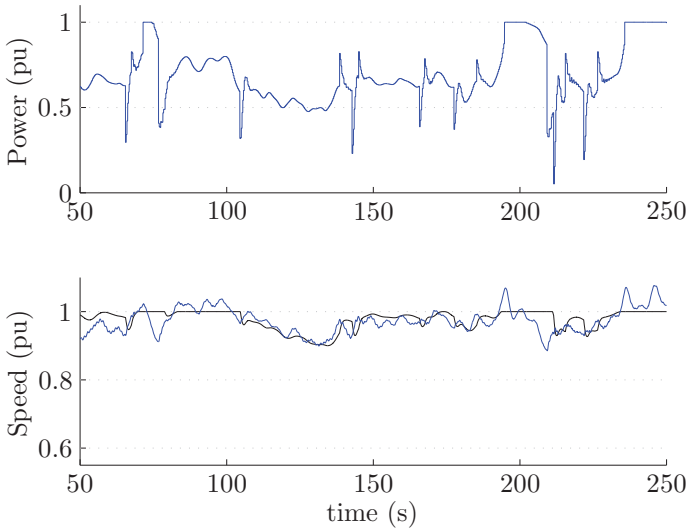

Figure 8: Simulation of wind turbine with instantaneous change between controllers. This simulation is based on the same wind speed profile as in Figure 7, and shows output power (top) and turbine rotational speed (bottom).

It should be noted at this point that the second case with sudden controller change (Figure 8) has been presented only to illustrate the difference, and is not a considered a realistic control system alternative as no parameter tuning has been done to get the best behaviour.

6. Conclusion

This paper has presented a wind turbine control system with smooth behaviour during transitions between controllers. The smooth behaviour is achieved by weighting factors that depend on the wind speed and give a gradual transition from one controller to another, i.e. a bumpless transfer. The main aim of this paper has been to describe this new control concept and to give an example of its application.

The explicit control system implementation discussed in this paper has been designed for an offshore floating wind turbine, using a 5-mass model of the turbine and a 6-DOF model of the floating tower. The control system was chosen to use a linear Model Predictive Control approach. Different MPC controllers were defined around different operating points, with overall smooth behaviour ensured by the bumpless transfer approach.

It should be pointed out that although the example in this paper uses an MPC approach, the bumpless transfer algorithm is general and could easily be applied with other types of controllers, or even a mix of different types of controllers.

Simulations have been performed to demonstrate the bumpless transfer characteristics as well as the tower stability of the floating wind turbine.

Regarding tower stability, these simulations have demonstrated that the suggested control system gives a stabilisation of tower oscillations. In the MPC approach used here, this is essentially achieved simply by using a prediction horizon that exceeds the periodicity of the tower oscillations. Since tower oscillations have a low frequency, this has the downside that it requires a relatively large prediction horizon, and therefore gives relatively high computational requirements. It has not been discussed whether this might be a problem for practical implementation.

Regarding bumpless transfer, the simulations have clearly demonstrated that the system using the proposed algorithm for smooth transition indeed exhibits a smooth system behaviour. In comparison to a case with sudden transition, the behaviour is significantly improved.

Smooth system behaviour is important to increase the lifetime of critical parts of the turbine. With increasing turbine sizes such considerations are of increasing importance, making the results obtained in this paper of particular relevance for large wind turbines, both onshore and offshore.

Acknowledgements

We are grateful to Karl Merz and John Olav Tande for useful comments on the manuscript, and to Thor Inge Fossen for help in generating WAMIT output. The writing of this paper has been funded through the Norwegian Research Centre for Offshore Wind Technology (NOWITECH).

References

[1] EWEA, Pure Power – Wind energy targets for 2020 and 2030, EWEA, 2011.
[2] Blue H (Accessed July 2011). [link].
URL www.bluehgroup.com
[3] Statoil, Hywind (Accessed July 2011).
URL www.statoil.com
[4] Sway (Accessed September 2011). [link].
URL www.sway.no
[5] Principle Power, Windfloat (Accessed September 2011).
URL www.principlepowerinc.com
[6] J. Maciejowski, Predictive Control with Constraints, Prentice-Hall, 2002.
[7] M. Nikolaou, Model predictive controllers: A critical synthesis of theory and industrial needs, in: Advances in Chemical Engineering, Vol. 26, Academic Press, 2001, pp. 131 – 204. doi:10.1016/S0065-2377(01)26003-7.
[8] L. C. Henriksen, Model predictive control of a wind turbine, Master's thesis, Technical University of Denmark (2007).
[9] M. Khalid, A. V. Savkin, A model predictive control approach to the problem of wind power smoothing with controlled battery storage, Renweable Energy 35 (2010) 1520 – 1526. doi:10.1016/j.renene.2009.11.030.
[10] A. Kusiak, W. Li, Z. Song, Dynamic control of wind turbines, Renweable Energy 35 (2010) 456 – 463. doi:10.1016/j.renene.2009.05.022.
[11] E. B. Muhando, T. Senjyu, N. Urasaki, A. Yona, T. Funabashi, Robust predictive control of variable-speed wind turbine generator by self-tuning regulator, in: Power Engineering Society General Meeting, 2007. IEEE, 2007. doi:10.1109/PES.2007.385885.
[12] T. K. A. Brekken, On model predictive control for a point absorber wave energy converter, in: IEEE PES Trondheim PowerTech, 2011. doi:10.1109/PTC.2011.6019367.
[13] E. Lindeberg, Optimal control of floating offshore wind turbines, Master's thesis, Norwegian University of Science and Technology, Department of Engineering Cybernetics (2009).
URL http://urn.kb.se/resolve?urn=urn:nbn:no:ntnu:diva-9933
[14] M. Chinchilla, S. Arnaltes, J. Burgos, Control of permanent-magnet generators applied to variable-speed wind-energy systems connected to the grid, IEEE Transactions on Energy Conversion 21 (2006) 130 – 135. doi:10.1109/TEC.2005.853735.
[15] C. Nichita, D. Luca, B. Dakyo, E. Ceanga, Large band simulation of the wind speed for real time wind turbine simulators, Energy Conversion, IEEE Transactions on 17 (4) (2002) 523–529. doi:10.1109/TEC.2002.805216.
[16] Wamit Inc, WAMIT (Accessed July 2011).
URL www.wamit.com
[17] T. I. Fossen, Handbook of Marine Craft Hydrodynamics and Motion Control, Wiley, 2011.
[18] MSS. marine systems simulator (2010) (Accessed 1 Jul 2011).
URL http://www.marinecontrol.org
[19] T. Larsen, T. Hanson, A method to avoid negative damped low frequent tower vibrations for a floating, pitch controlled wind turbine, Journal of Physics: Conference Series 75 (2007) 012073. doi:10.1088/1742-6596/75/1/012073.
[20] J. Jonkman, Influence of control on the pitch damping of a floating wind turbine, conference Paper NREL/CP-500-42589, National Renewable Energy Laboratory, Golden, CO, USA, 2008; presented at the 2008 ASME Wind Energy Symposium, Reno, NV, USA, January 7-10 (2008).
[21] F. G. Nielsen, B. Skaare, J. O. G. Tande, I. Norheim, K. Uhlen, Method for damping tower vibrations in a wind turbine installation, patent (2008).
URL www.google.com/patents/US20080260514
[22] B. Skaare, Method for the damping of tower oscillations in wind power installations, patent (2009).
URL www.google.com/patents/US20100045038
[23] M. Lackner, Controlling platform motion and reducing blade loads for floating wind turbines, Wind Engineering 33 (2009) 541–553. doi:10.1260/0309-524X.33.6.541.
[24] M. Karimirad, T. Moan, Ameliorating the negative damping in the dynamic responses of a tension leg spar-type support structure with a downwind turbine, presented at the European Wind Energy Conference, Brussels, Belgium, March 14-17 (2011).
[25] H. Namik, K. Stol, Individual blade pitch control of floating offshore wind turbines, Wind Energy 13 (1) (2010) 74–85. doi:10.1002/we.332.

[26] H. Namik, K. Stol, Performance analysis of individual blade pitch control of offshore wind turbines on two floating platforms, Mechatronics 21 (4) (2011) 691–703. doi:10.1016/j.mechatronics.2010.12.003.

[27] S. Christiansen, T. Knudsen, T. Bak, Optimal control of a ballast-stabilized floating wind turbine, in: IEEE International Symposium on Computer-Aided Control System Design (CACSD), Denver, CO, USA, September 28-30, 2011, pp. 1214–1219. doi:10.1109/CACSD.2011.6044574.

[28] S. Trollnes, et al., Hywind: Two years in operation, what have we learnt and where are we going?, presented at the 9th Deep Sea Offshore Wind R&D Seminar, Trondheim 25 Jan 2012.
URL http://www.sintef.no/Projectweb/Deepwind%5F2012/Presentations